Chemistry Letters

Temperature Effects on the Photovoltaic Performance of Planar Structure Perovskite Solar Cells

Ludmila Cojocaru,* Satoshi Uchida,* Yoshitaka Sanehira, Victoria Gonzalez-Pedro, Juan Bisquert, Jotaro Nakazaki, Takaya Kubo, and Hiroshi Segawa*

Temperature Effects on the Photovoltaic Performance of Planar Structure Perovskite Solar Cells

Ludmila Cojocaru[1], Satoshi Uchida[2], Yoshitaka Sanehira[3], Victoria Gonzalez-Pedro[4], Juan Bisquert[4,5], Jotaro Nakazaki[1], Takaya Kubo[1] and Hiroshi Segawa[1]

[1]*Research Center for Advanced Science and Technology, The University of Tokyo, Komaba 4-6-1, Meguro-ku, Tokyo 153-8904*
[2]*Komaba Organization for Educational Excellence, The University of Tokyo, Komaba 3-8-1, Meguro-ku, Tokyo 153-8902*
[3]*Graduate School of Engineering, Toin University of Yokohama, Kurogane-cho 1614, Aoba-ku, Yokohama 225-8503*
[4]*Institute of Advanced Materials (INAM), Universitat Jaume I,12006 Castelló, Spain*
[5]*Department of Chemistry, Faculty of Science, King Abdulaziz University, Jeddah, Saudi Arabia*

E-mail: cojocaru@dsc.rcast.u-tokyo.ac.jp, uchida@rcast.u-tokyo.ac.jp, csegawa@mail.ecc.u-tokyo.ac.jp

Temperature effects of $CH_3NH_3PbI_3$ perovskite solar cells having simple planar architecture were investigated on the crystal structure and photovoltaic performance. The obvious changes in the $CH_3NH_3PbI_3$ crystal structure were found by varying the temperature as a consequence to the augmentation in lattice parameters and expansion of unit cell. The expansion of the crystal gave a serious influence on the performance of the solar cells, where the differences in the coefficients of the thermal expansion (CTEs) together with the lattice mismatch between TiO_2 and perovskite materials might cause interfacial defects responsible for the deterioration in the photovoltaic performance. Interestingly, the hysteresis in the cubic phase is very small because of the less distorted angles of the $CH_3NH_3PbI_3$ structure against the temperature fluctuation.

Perovskite solar cells based on $CH_3NH_3PbI_3$ have attracted enormous attention in the last few years[1] due to their rapid improvement and high certified efficiencies over 20%.[2] The architectures of the devices have been categorized to mesoscopic structure or simple planar heterojunction[3] and the devices exhibit large hysteresis in J-V characteristics especially in the planar structure.[4] The solar cells presents a big mismatch in the power conversion efficiency (PCE) from forward (short circuit to open circuit) and reverse scan (open circuit to short circuit), and correct estimation of the PCE has been a controversial matter in recent past.[5] Several hypotheses have been proposed to be the origin of the hysteresis in planar architecture, such as ferroelectric proprieties of $CH_3NH_3PbI_3$,[6] ion migration inside perovskite layer,[7] chemical and structural changes in the materials, and interfacial contact between the layers.[8] However, the mechanism responsible of the anomalous hysteresis remains unclear.

Another possible factor of the hysteresis is the interfacial contact and lattice mismatch between compact TiO_2 and perovskite layer.[9] This interface may cause the temporal delay of the J-V characteristics due to rearrangement of the interface under external bias and illumination. In fact, large decrease of hysteresis has been shown by modification of the compact TiO_2 layer using fullerene derivatives (C_{60}, 60-PCBM).[10] In this case, there is no lattice mismatch as the inorganic interface of the crystalline. Petrozza et al.[10b] also showed that allowing the TiO_2 interface to rearrange under voltage bias, produces a similar injection rate to that of PCBM contact. One factor that affects the interfacial properties is ion accumulation, as shown by the large capacitance associated to

electrode polarization.[11] From theoretical calculation, it has been found that migration of defects originated from diffusion of iodide vacancies or high orientation of $CH_3NH_3^+$, is able to modify the interface.[12] In addition, $CH_3NH_3PbI_3$ undergoes several crystal phase transitions when temperature of the solar cell is changed.[13] Recently, several devices with PCBM were investigated at low temperature.[14] However there is no clear evidence showing effect of temperature on the connection between structural transformation and photovoltaic response of devices and magnitude of hysteresis.

In this study, we investigated structural changes of planar heterojunction perovskite solar cells at different temperatures by the use of an in-situ X-ray diffraction analysis (Bruker, D8 Discover X-ray Diffractometer operates at 40 kV). In order to avoid water condensation from the air at low temperatures and contamination of the perovskite film, the devices were put inside a domed cooling stage (Anton Paar, DSC 350). Solar cell devices of planar structure[15] were prepared using compact TiO_2 layer as electron-extracting layer. The perovskite films were prepared using mixed halide precursor solution containing $PbCl_2$ and CH_3NH_3I by one-step deposition method. After annealing the perovskite layer, the final compound formed is essentially $CH_3NH_3PbI_3$ although a trace amount of chloride can be found in the device.[16] Finally, the hole transport layer was deposited on the perovskite layer.

The XRD pattern of $CH_3NH_3PbI_3$ without bias voltage in the dark was measured under standard conditions at room temperature (Figure S1). The characteristic peaks at 14.1°, 28.5° and 43.3° are attributed to the (110), (220) and (330) planes confirm the tetragonal I4/*mcm* space group at room temperature. The shoulder peak at 14.3° aside of (110) peak was assigned to (002) peak as shown in Figure S2.[13a] All the characteristic XRD peaks (110), (002), (220) and (330) shifted to lower angle when temperature of the samples increased from -95 °C to +100 °C (Figure S2). The left angle shift of the peaks can be interpreted to augmentation of lattice spacing with temperature and this behavior is ascribed to the tetragonal to cubic transition.[13b] Moreover, we observed no change in XRD pattern of perovskite solar cells measured under different light intensities and applied voltages (Figure S3 (a,b)), and keeping the temperature constant at 25 °C.

In order to calculate the lattice parameters *a* and *c* from XRD pattern the 2θ was converted to *d* value and using Bragg's law. Using *d* value of the peaks (110) (002), and the

plane spacing equation[17], we calculated the values of lattice parameters *a* and *c*, respectively (Figure 1). Tetragonal lattice parameters were converted to pseudo-cubic parameters.[13a] The unit cell volume calculated from the lattice parameters depends linearly on temperature and shows a clear continuous change. $CH_3NH_3PbI_3$ changes from the tetragonal to cubic phase at +55 ºC. These results matched with previous works[13a] with slight difference in the phase transition temperature.
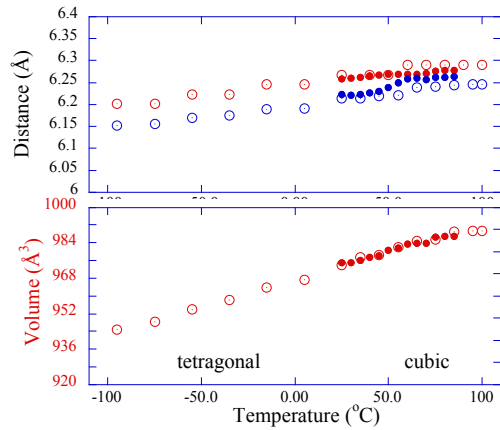
Figure 1. Lattice parameters and unit cell volume obtained from X-ray diffraction analysis of $CH_3NH_3PbI_3$ based solar cells. (a* parameters red dots and c* parameters blue dots) solid dots and is reference data published in ref 13a.

It is well known that the response of solids at different temperature is expressed as its coefficient of thermal expansion (CTE).[18] The coefficient is also known as the thermal expansion, expressing the rate of change of the unit volume with temperature. The thermal expansion is characterized by two coefficients, the linear and volumetric thermal expansion. The volumetric thermal expansion coefficient can be estimated as:

$$\alpha_V = \frac{1}{V}\left(\frac{\partial V}{\partial T}\right)$$

where α_V is CTE, V is the volume of the material and $\partial V/\partial T$ the rate of change of that volume with temperature. Numerous previous studies, using a large variety of sample compositions have been carried out for determination of CTE. Based on those results, the calculated volumetric CTE for related materials of perovskite solar cells are shown in Table 1.[18] The volumetric CTE extracted from the experimental XRD plotted in Figure 1 at the range 173-328K (temperature range for tetragonal structure) is 216×10^{-6} K^{-1} and at the range 338-373K (temperature range for cubic structure) is 88×10^{-6} K^{-1}. The calculated CTE for $CH_3NH_3PbI_3$ in this work is closer to the data already reported by another group.[18e] The bond mismatch also contributes the interconnectivity between TiO_2 and $CH_3NH_3PbI_3$ materials (Figure S4). The example of imperfect connections (gaps) between layers in special at the interface compact TiO_2 and $CH_3NH_3PbI_3$ layer was shown in Figure S5.

Table 1. The volumetric CTE for materials used in perovskite solar cells. The $CsSnI_3$ (PbTe)[18] is used as reference for $CH_3NH_3PbI_3$.

Materials	(CTE)/$\times 10^{-6}$ K^{-1}
$CH_3NH_3PbI_3$	132 (300 K)[18e]
	216 (173-328K) this work
	88 (338-373 K) this work
$CsSnI_3$	126 (300 K)[18c]
PbTe	70 (300 K)[18d]
TiO_2 (Anatase)	23.5 (300 K)[18a]
SnO_2	11.7 (300 K)[18b]

In the current voltage (J-V) measurements on perovskite solar cells under N_2 atmosphere at different temperatures (Figure 2 from -40 °C to +100 °C), the temperature was monitored in the chamber and on the top surface of the perovskite solar cells. The scan voltage range was fixed from +1.2 V to -0.05 V, starting from positive voltage for reverse scan and from negative voltage for forward scan. The J-V measurement was started from +25 °C for two devices with similar initial PCE, one for negative temperature scanning from +25 to -95°C and another for positive temperature scanning from +25 to +100°C.
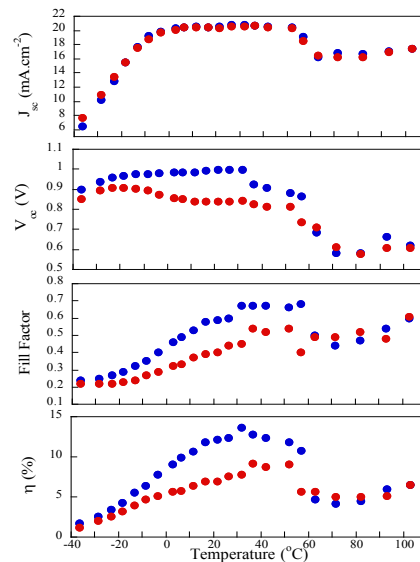
Figure 2. Photovoltaic parameters (J_{sc}, V_{oc}, FF and η) for $CH_3NH_3PbI_3$ based perovskite solar cells as a function of temperature. (red dots for forward scan and blue dots for reverse scan).

These results are in good agreement with previous studies reported in the literature.[19] Three J-V curves with photovoltaic parameters at +25, -40 and +100°C are shown in the Figure S6 (Table S1 for full devices parameters). In the photovoltaic parameters at different temperatures, the hysteresis is observed at the temperature range of -20 °C to +55 °C and the mismatch within the forward and reverse scan is mainly attributed to the differences in V_{oc} and FF.[15] In the temperature range between -40 and -20 ºC, the low photovoltaic performance is associated with the reduced diffusion of photocarriers which is reflected in lower FF values. On the other hand, the maximum photoconversion efficiency was observed in the range from 20 to 40 ºC (the best at temperature 30 ºC in the reverse scan, J_{sc}=20.6 mA cm⁻

3

^{2}, V_{oc}=0.996 V, FF=0.67, PCE=13.6 %) with hysteric effect (in the forward scan J_{sc}=20.8 mA cm^{-2}, V_{oc}=0.842 V, FF=0.45, PCE=7.8 %). Additionally, we observed a drop in photovoltaic performance at around +55 °C corresponding to the phase transition of perovskite from tetragonal to cubic. The adhesion of films to the substrates is critical in the systems where the CTEs are different. In this context, the interfacial connectivity in the TiO$_2$/CH$_3$NH$_3$PbI$_3$ interface determines the goodness of the contact. The CTE of CH$_3$NH$_3$PbI$_3$ is 5.6 times higher than that of TiO$_2$ (Table1), which may cause stress and delamination resulting in an increase in the interfacial defects and poor interconnectivity between the two layers. This fact together with the faster recombination processes at high temperature produces a variation in the density of states which is reflected in the drop of photovoltage at high temperatures. Moreover, the higher recombination reduces the photocarrier diffusion length an increases the total series resistance that is reflected in the lower FF values.[20]

On the other hand, analyzing the forward and reverse scan, it is noteworthy the lack of hysteresis in the cells after the phase transition (temperature > +55°C). It was found that rapid orientation of CH$_3$NH$_3$$^+$ is strongly affected by change in the temperature.[13a] A similar trend is expected in case of the mobility of the I$^-$ which is also considered most mobile species in CH$_3$NH$_3$PbI$_3$.[12a] Another group[12b] reported that with increasing temperature the [PbI$_3$]$^-$ framework becomes less distorted and CH$_3$NH$_3$$^+$ undergoes larger atomic displacement and migrates to the center of the perovskite cube, resulting in the formation of cubic structure at +55 °C. Due to the movement of the CH$_3$NH$_3$$^+$ in the perovskite crystal [PbI$_3$]$^-$ framework gets deformed. In the tetragonal structure, the interaction between NH$_3$ and [PbI$_3$]$^-$ framework becomes weaker with increasing temperature and very week at room temperature. Before cubic phase transition, at the temperature closer to room temperature, the NH$_3$ and CH$_3$ group become free, resulting in the straightening of the Pb-I-Pb bonds, with angle of 165.3°. In the cubic structure, the CH$_3$NH$_3$$^+$ becomes orientaly disordered and the angle Pb-I-Pb becomes 180°. The lack of angle distortion in the cubic framework can affect the ionic rearrangement processes responsible of the hysteresis. We observe the reversibility on the shift of the XRD peaks and J-V measurement as shown in Figure S7.

In conclusion, it was observed that perovskite unit cell volume increases linearly with temperature and the divergence in the CTE within CH$_3$NH$_3$PbI$_3$ and TiO$_2$ affects the interfacial connectivity after thermal treatment. Regarding the hysteresis, the big difference in the J-V measurement, for reverse and forward scan is observed from 0 to +55° C. We attribute this fact to the less distorted Pb-I-Pb angle in the cubic phase (temperature >+55 ℃), which have a direct role in the internal rearrangement processes in the perovskite layer. In this regard, the better understanding of the hysteresis in planar structure perovskite based solar cells and the improvement of the interlayer connectivity with selective contact may considered a good route for the development of robust and high performance perovskite solar cells.

References and Notes

1   a) A. Kojima, K. Teshima, Y. Shirai, T. Miyasaka, *J. Am. Chem. Soc.* **2009**, *131*, 6050. b) M. M. Lee, J. Teuscher, T. Miyasaka, T. N. Murakami, H. J. Snaith, *Science* **2012**, *338*, 643. c) J. Burschka, N. Pellet, S. J. Moon, R. Humphry-Baker, P. Gao, Md. K. Nazeeruddin, M. Grätzel *Nature* **2013**, *499*, 316. d) T. Miyasaka, *ChemLett.* **2015**, doi:10.1246/cl.150175.

2   M. A. Green, K. Emery, Y. Hishikawa, W. Warta, E. D. Dunlop, *Prog. Photovolt: Res. Appl.* **2015**, *23*, 1.

3   M. Liu, M. B. Johnston, H. J. Snaith, *Nature* **2013**, *501*, 395.

4   H. J. Snaith, A. Abate, J. M. Ball, G. E. Eperon, T. Leijtens, N. K. Noel, S. D. Stranks, J. Tse-Wei Wang, K. Wojciechowski, W. Zhan, *J. Phys. Chem. Lett.* **2014**, *5(9)*, 1511.

5   a) E. Zimmermann, P. Ehrenreich, T. Pfdaler, J. A. Dorman, J. Weickert, L. Schmidt-Mende, *Nature Photonics* **2014**, *8*. 669. b) M. Grätzel, *Nature Materials* **2014**, *13*, 838. c) M. D. McGehee, *Nature Materials* **2014**, *13*, 845. d) Editorial, *Nature Materials* **2014**, *13*, 837.

6   H. W. Chen, N. Sakai, M. Ikegami, T. Miyasaka, *J. Phys. Chem. Lett.* **2014**, *6*, 164.

7   E. L. Unger, E. T. Hoke, C. D. Bailie, W. H. Nguyen, A. R. Bowring, T. Heumuller, M. G. Christoforo, M. D. McGehee, *Energy Environ. Sci.* **2014**, *7*, 3690.

8   A. K. Jena, H. W. Chen, A. Kogo, Y. Sanehira, M. Ikegami, T. Miyasaka, *ACS Appl. Mater. Interfaces,* **2015**, *7(18)*, 9817.

9   J. Shi, X. Xu, D. Li, Q. Meng, *Small* **2015**, doi: 10.1002/smll.201403534.

10   a) K. Wojciechowski, S. D. Stranks, A. Abate, G. Sadoughi, A. Sadhanala, N. Kopidakis, G. Rumbles, C. Z. li, R. H. Friend, A. K. –Y. Jen, H. J. Snaith, *ACS Nano*, **2014**, *8*, 12701. b) C. Tao, S. Neutzner, L. Colella, S. Marras, A. R. S. Kandada, M. Gardini, M. De Bastiani, G. Pace, L. Manna, M. Caironi, C. Bertarelli, A. Petrozza, *Energy Environ. Sci.* **2015**, *8*, 2365.

11   O. Almora, I. Zarazua, E. Mas-Marza, I. Mora-Sero, J. Bisquert, G. Garcia-Belmonte. *J. Phys. Chem. Lett.* **2015**, *6(9)*, 1645.

12   a) J. M. Azpiroz, E. Mosconi, J. Bisquert, F. De Angelis, *Energy Environ. Sci.,* **2015**, *8,* 2118. b) M. T. Weller, O. J. Weber, P. F. Henry, A. M. Di Pumpo, T. C. Hansen, *Chem. Commun.*, **2015**, *51*, 4180.

13   a) T. Baikie, Y. Fang, J. M. Kadro, M. Schreyer, F. Wei, S. G. Mhaisalkar, M. Gratzel, T. J. White. *J. Mater. Chem. A*, **2013**, *1*, 5628. b) Y. Kawamura, H. Mashiyama, K. Hasebe, *J. Phys. Soc. of Japan*, **2002**, *71(7)*, 1694.

14   D. Bryant, S. Wheeler, B. C. O'Regan, T. Watson, P. R. F. Barnes, D. Worsley, J. Durrant, *J. Phys. Chem. Lett.* **2015**, *6*, 3190.

15   L. Cojocaru, S. Uchida, Y. Sanehira, J. Nakazaki, T. Kubo, H. Segawa, *ChemLett.* **2015**, *44(5)*, 674.

16   L. Cojocaru, S. Uchida, A. K. Jena, T. Miyasaka, J. Nakazaki, T. Kubo, H. Segawa, *ChemLett.* **2015**, *44(8),* 1089.

17   Y. Waseda, E. Matsubara, K. Shinoda. X-Ray diffraction crystallography. Introduction, examples and solved Problems. Doi 10.1007/978-3-642-16635-8.

18   a) A. Mashreghi, *Computational Materials Science* **2012**, *62,* 60. b) P. S. Percy, B. Morosin, *Phys. Rev.* **1973**, *B7*, 2779. c) I. Chung, J. –H. Song, J. Im, J. Androulakis, C. D. Malliakas, H. Li, A. J. Freeman, J. T. Kenney, M. G. Kanatzidis, *J. Am. Chem. Soc.* **2012**, *134*, 8579. d) J. M. Skelton, S. C. Parker, A. Togo, I. Tanaka, A. Walsh, *Phys. Rev. B,* **2014**, *89*, 205203. e) F. Brivio, J. M. Frost, J. M. Skelton, A. J. Jackson, O. J. Weber, M. T. Weller, A. Walsh, arXiv preprint arXiv:1504.07508

19   a) L. K. Ono, S. R. Raga, S. Wang, Y. Kato, Y. Qi, *J. Mater. Chem. A*, **2015**, *3*, 9074. b) E. A. Katz, D. Faiman, S. M. Tuladhar, *J. Appl. Phys.* **2001**, *90 (10)*, 5343. c) D. M-Rodriquez, P. P. Horley, J. Gonzalez-Hernandez, Y. V. Vorobiev, P. N. Gorley, *Solar Energy* **2005**, *78* (2), 243.

20   a) F. Fabregat-Santiago, G. Garcia-Beltimonte, I. Mora-Sero, J. Bisquert, *Phys. Chem. Chem. Phys.* **2011**, *13*, 9083. b) S. R. Raga, E. M. Barea, F. Fabregat-Santiago, *J. Phys. Chem. C*, **2012**, *3(12)*, 1629.